Lilly, J. M., & Olhede, S. C. (2009). Wavelet ridge estimation of jointly modulated multivariate oscillations. Published in *2009 Conference Record of the Forty-Third Asilomar Conference on Signals, Systems and Computers*, 452–456. November 14, 2009, Pacific Grove, CA, USA.

Wavelet ridge estimation of jointly modulated multivariate oscillations

(Invited Paper)

Jonathan M. Lilly
Earth and Space Research
2101 Fourth Ave., Suite 1310
Seattle, WA 98121, USA
Email: lilly@esr.org

Sofia C. Olhede
Department of Statistical Science
University College London
Gower Street, London WC1 E6BT, UK
Email: s.olhede@ucl.ac.uk

***Abstract*—Wavelet ridge analysis is a technique for estimating the time-varying properties of a modulated oscillatory signal from a contaminated observation. Here this technique is extended to the multivariate case, that is, to a set of N real-valued time series. The bivariate case is illustrated with an application to a set of freely-drifting oceanographic floats. A freely distributed software package implementing this algorithm is available online at http://www.jmlilly.net.**

I. Introduction

A wide variety of signals may be characterized as *modulated oscillations*, represented in the form

$$x(t) = a(t)\cos\phi(t) \tag{1}$$

where $a(t)$ is a time-varying amplitude and $\phi(t)$ is a time-varying phase. While the choice of amplitude and phase is not unique, there is a special amplitude/phase pair—the *canonical pair* $a_+(t)$, $\phi_+(t)$—that is of particular interest [1]. A typical observation $x^{(o)}(t)$ of this modulated oscillation will not appear in isolation, but will be contaminated by other signal components or noise, that is,

$$x^{(o)}(t) = x(t) + x^{(\varepsilon)}(t) \tag{2}$$

where $x^{(\varepsilon)}(t)$ is some kind of "noise" process. An important task is then to estimate the modulated oscillation $x(t)$, and the canonical pair, from the contaminated observation $x^{(o)}(t)$.

An attractive solution to this problem is *wavelet ridge analysis* [2], [3]. From the observation $x^{(o)}(t)$, this method gives an estimate $\widehat{x}(t)$ of a modulated oscillation $x(t)$ which is relatively insensitive to the noise process $x^{(\varepsilon)}(t)$. This insensitivity is due to the localizing nature of the analyzing function or *wavelet* that is applied to the observed signal.

Often one wishes to analyze not a single univariate modulated oscillation $x(t)$, but a set of real-valued signals,

$$\mathbf{x}(t) = \begin{bmatrix} x_1(t) \\ x_2(t) \\ \vdots \\ x_N(t) \end{bmatrix} = \begin{bmatrix} a_1(t)\cos\phi_1(t) \\ a_2(t)\cos\phi_2(t) \\ \vdots \\ a_N(t)\cos\phi_N(t) \end{bmatrix} \tag{3}$$

The work of J. M. Lilly was supported by award #0526297 from the Physical Oceanography program of the United States National Science Foundation.

with the N canonical amplitude/phase pairs $a_n(t)$, $\phi_n(t)$ describing each of the N component signals as a modulated oscillation. The most important multivariate cases are $N = 2$ and $N = 3$. The bivariate case, which encompasses complex-valued signals, is common in oceanography and atmospheric science, see [4] and references therein, while the trivariate case is central to seismology [5]–[7].

The purpose of this paper is to present a version of wavelet ridge analysis appropriate for multivariate signals of the form (3). This builds on recent works by the authors: (i) the examination of the bias of wavelet ridge analysis—that is, its behavior in the absence of noise—for a univariate signal [8], and (ii) the extension of the notions of instantaneous moments to accommodate a multivariate signal [9].

II. Representation

The first step is to obtain a representation of a modulated multivariate oscillation. As in the univariate case [1], [10], [11], a unique representation is specified by taking the analytic part of the vector-valued signal. Following [9], an instantaneous quantity may then be found which integrates to the first moment of the aggregate spectrum of the signal, generalizing the univariate instantaneous frequency [10]–[12] to the multivariate case. The complex-valued *analytic signal vector* is defined as

$$\mathbf{x}_+(t) \quad \equiv \quad 2\mathcal{A}[\mathbf{x}](t) \equiv \mathbf{x}(t) + i\frac{1}{\pi}⨍_{-\infty}^{\infty}\frac{\mathbf{x}(u)}{t-u}\,du \tag{4}$$

where "$⨍$" is the Cauchy principal value integral and $\mathcal{A}$ is called the *analytic operator*. A set of N unique amplitudes and phases, called the *canonical set*, is defined in terms of the analytic vector via

$$\begin{aligned}\mathbf{x}_+(t) &\equiv \begin{bmatrix} x_{+;1}(t) & x_{+;2}(t) & \dots & x_{+;N}(t) \end{bmatrix}^T \\ &\equiv \begin{bmatrix} a_1(t)e^{i\phi_1(t)} & a_2(t)e^{i\phi_2(t)} & \dots & a_N(t)e^{i\phi_N(t)} \end{bmatrix}^T \end{aligned} \tag{5}$$

with $a_n(t) \equiv |x_{+;n}(t)|$ and $\phi_n(t) \equiv \arg\{x_{+;n}(t)\}$; here "arg" denotes the complex argument and "T" is the matrix transpose. This is simply the application of the definition of the canonical amplitude and phase to the components of a multivariate time series.

The analytic operator has a very simple form in the frequency domain. The signal vector $\mathbf{x}(t)$ is expressed in terms of its Fourier transform $\mathbf{X}(\omega)$ as

$$\mathbf{x}(t) = \frac{1}{2\pi}\int_{-\infty}^{\infty} e^{i\omega t}\,\mathbf{X}(\omega)\,d\omega \tag{6}$$

while the analytic signal vector is similarly given by

$$\mathbf{x}_+(t) = \frac{1}{2\pi}\int_{-\infty}^{\infty} e^{i\omega t}\,\mathbf{X}_+(\omega)\,d\omega \tag{7}$$

where we have introduced

$$\mathbf{X}_+(\omega) \equiv 2U(\omega)\mathbf{X}(\omega) \tag{8}$$

with $U(\omega)$ being the unit step function. Thus the action of the operator $2\mathcal{A}[\mathbf{x}](t)$ is to double the amplitudes of the Fourier coefficients of $\mathbf{X}(\omega)$ at positive frequencies, while causing the coefficients at negative frequencies to vanish.

The real-valued signal vector $\mathbf{x}(t)$ is expressed in terms of the analytic signal vector $\mathbf{x}_+(t)$ by $\mathbf{x}(t) = \Re\,\{\mathbf{x}_+(t)\}$. The vector $\mathbf{x}(t)$ can now be described, via (3), as a set of N modulated oscillations having unique amplitude and phase functions. Since a wide variety of physical processes can be usefully described as modulated multivariate oscillations, (3) is a powerful representation for the structure of a vector-valued signal. The construction of the analytic signal vector thus permits a unique description of a multivariate signal as a *modulated multivariate oscillation*.

The aggregate frequency-domain structure of the analytic vector $\mathbf{x}_+(t)$ is described by the *joint analytic spectrum*

$$S_{\mathbf{x}}(\omega) \quad \equiv \quad \mathcal{E}_{\mathbf{x}}^{-1}\|\mathbf{X}_+(\omega)\|^2 \tag{9}$$

where $\|\mathbf{x}\| \equiv \sqrt{\mathbf{x}^H\mathbf{x}}$ is the norm of some complex-valued vector $\mathbf{x}$, "H" indicating the conjugate transpose, and where

$$\mathcal{E}_{\mathbf{x}} \equiv \frac{1}{2\pi}\int_0^{\infty}\|\mathbf{X}_+(\omega)\|^2 d\omega = \int_{-\infty}^{\infty}\|\mathbf{x}_+(t)\|^2 dt \tag{10}$$

is the total energy of the multivariate analytic signal. $S_{\mathbf{x}}(\omega)$ is the average of the spectra of the N analytic signals, normalized to unit energy. The *joint global mean frequency*

$$\overline{\omega}_{\mathbf{x}} \equiv \frac{1}{2\pi}\int_0^{\infty}\omega S_{\mathbf{x}}(\omega)\,d\omega \tag{11}$$

is clearly a measure of the average frequency content of the multivariate signal $\mathbf{x}(t)$.

The *joint instantaneous frequency* $\omega_{\mathbf{x}}(t)$ is then some quantities which decomposes $\overline{\omega}_{\mathbf{x}}$, across time, i.e. which satisfies

$$\overline{\omega}_{\mathbf{x}} = \mathcal{E}_{\mathbf{x}}^{-1}\int_{-\infty}^{\infty}\|\mathbf{x}_+(t)\|^2\,\omega_{\mathbf{x}}(t)\,dt \tag{12}$$

noting that $\|\mathbf{x}_+(t)\|^2$ is aggregate instantaneous power of the analytic signal vector. Although the integrand in this expression is non-unique, [9] shows that the definition

$$\omega_{\mathbf{x}}(t) \equiv \frac{\Im\left\{\mathbf{x}_+^H(t)\frac{d}{dt}\mathbf{x}_+(t)\right\}}{\|\mathbf{x}_+(t)\|^2} \tag{13}$$

satisfies (12), and is the natural generalization of the standard univariate definition of instantaneous frequency [10].

III. Multivariate wavelet ridge analysis

The identification and extraction of a modulated univariate oscillation from an observed time series may be accomplished by wavelet ridge analysis [2], [3]. Beginning with an analytic wavelet transform, a set of special points called *ridge points* are defined, which are then organized into contiguous curves called *ridge curves*. The set of values taken by a suitably normalized version of the wavelet transform constitute an estimator of a presumed modulated oscillation. The effect of noise on the transform behavior is beyond the scope of this paper, and so for simplicity we assume here that the modulated oscillation is uncontaminated, i.e. that $\mathbf{x}(t) = \mathbf{x}^{\{o\}}(t)$.

Building on the results of the previous section, wavelet ridge analysis can be extended to the multivariate case. Here we will closely follow the development of [8] for the univariate case. As usual, a wavelet $\psi(t)$ is a zero-mean, square-integrable function, satisfying the "admissibility condition" [13]

$$\int_{-\infty}^{\infty}\frac{|\Psi(\omega)|^2}{|\omega|}\,d\omega \quad < \quad \infty \tag{14}$$

where $\Psi(\omega)$ is the Fourier transform of the wavelet; we consider only analytic wavelets, that is, wavelets $\psi(t)$ having no support on negative frequencies. The analytic wavelet transform of a signal $x(t) \in L^2(\mathbb{R})$ is a series of time-domain filtrations

$$W_{\psi}(t,s) \equiv \int_{-\infty}^{\infty}\frac{1}{s}\,\psi^*\left(\frac{\tau - t}{s}\right)x(\tau)\,d\tau \tag{15}$$

where the asterisk denotes the complex conjugate, t is the time, and s is called the *scale*. For the vector-valued signal $\mathbf{x}(t)$ having N components, we then define

$$\mathbf{w}_{\psi}(t,s) \equiv \int_{-\infty}^{\infty}\frac{1}{s}\psi^*\left(\frac{\tau - t}{s}\right)\mathbf{x}(\tau)\,d\tau \tag{16}$$

as the corresponding vector-valued wavelet transform, an N-vector function of time and scale.

Note that we use a $1/s$ normalization rather than the more common $1/\sqrt{s}$, and also choose the maximum value of the wavelet—which occurs at the *peak frequency* $\omega = \omega_{\psi}$—to be $\Psi(\omega_{\psi}) = 2$. With these two choices, the wavelet transform of a univariate sinusoid $x(t) = a_o\cos(\omega_o t)$ conveniently obtains a largest absolute value at any scale at $s = \omega_{\psi}/\omega_o$, and this largest value is simply the magnitude of the sinusoid $|W_{\psi}(t, \omega_{\psi}/\omega_o)| = |a_o|$. The quantity ω_{ψ}/s expresses scale in units of frequency [14].

The detection of a modulated oscillation within the analytic wavelet transform $\mathbf{w}_{\psi}(t,s)$ is accomplished as follows. An *amplitude ridge point* of $\mathbf{w}_{\psi}(t,s)$ is a time/scale pair (t,s) satisfying the two conditions

$$\frac{\partial}{\partial s}\,\|\mathbf{w}_{\psi}(t,s)\| \quad = \quad 0 \tag{17}$$

$$\frac{\partial^2}{\partial s^2}\,\|\mathbf{w}_{\psi}(t,s)\| \quad < \quad 0. \tag{18}$$

An *amplitude ridge curve* $\widehat{s}^{\{a\}}(t)$ is then a contiguous function of time composed of a collection of ridge points, and which

is constrained to satisfy the continuity condition

$$\left| \frac{d}{dt}\, \widehat{s}^{\{a\}}(t) \right| < \infty \tag{19}$$

in order to exclude multiple values of scale at a particular time. The set of ridge points satisfying these conditions will specify a ridge curve over some time interval which we denote by $T^{\{a\}}$. The *ridge-based signal estimate* associated with the amplitude ridge is then given by

$$\widehat{\mathbf{x}}^{\{a\}}_{+;\psi}(t) \equiv \mathbf{w}_\psi\Big(t, \widehat{s}^{\{a\}}(t)\Big) \quad t \in T^{\{a\}} \tag{20}$$

which is the set of values taken by the wavelet transform along the ridge curve. This definition of the multivariate amplitude ridge is the natural generalization of that presented by [8] for the univariate case.

It remains to show that the estimate (20) can accurately recover the modulated oscillation $\mathbf{x}(t)$. A change of variables applied to (16), together with the substitution $\mathbf{x}(t) = \left[\mathbf{x}_+(t) + \mathbf{x}^*_+(t)\right]/2$, leads to

$$\mathbf{w}_\psi(t,s) = \frac{1}{2}\frac{1}{s}\int_{-\infty}^{\infty} \psi^*\left(\frac{\tau}{s}\right)\, \mathbf{x}_+(t+\tau)\, d\tau \tag{21}$$

where the contribution of $\mathbf{x}^*_+(t+\tau)$ vanishes on account of the analyticity of the wavelet. Writing $\mathbf{x}_+(t+\tau)$ as

$$\mathbf{x}_+(t+\tau) = e^{i\omega_{\mathbf{x}}(t)\tau}\left[e^{-i\omega_{\mathbf{x}}(t)\tau}\mathbf{x}_+(t+\tau)\right] \tag{22}$$

and Taylor-expanding the bracketed term in τ, one finds

$$\begin{aligned}&\mathbf{x}_+(t+\tau) = e^{i\omega_{\mathbf{x}}(t)\tau}\times \\ &\left\{\mathbf{x}_+(t) + \tau e^{-i\omega_{\mathbf{x}}(t)(t_\epsilon - t)}\left[\mathbf{x}'_+(t_\epsilon) - i\omega_{\mathbf{x}}(t)\mathbf{x}_+(t_\epsilon)\right]\right\}\end{aligned} \tag{23}$$

for some $t_\epsilon \in [t, t+\tau]$ at each value of τ. The residual term in (23)—the term proportional to τ—follows from the Lagrange form of the remainder in the Taylor series [15, p 880]. Note that the residual term in (23) vanishes at time t_ϵ when

$$\mathbf{x}'_+(t_\epsilon) = i\omega_{\mathbf{x}}(t)\mathbf{x}_+(t_\epsilon) \tag{24}$$

in which case the analytic signal vector locally behaves like a set of sinusoids all evolving at the same frequency $\omega_{\mathbf{x}}(t)$. When the signal is composed of a set of sinusoids having identical frequencies, the residual term in (23) vanishes everywhere.

The wavelet transform then becomes, inserting the Taylor-expanded expression for the signal (23) into (21),

$$\mathbf{w}_\psi(t,s) = \frac{1}{2}\mathbf{x}_+(t)\Psi\left(s\omega_{\mathbf{x}}(t)\right) + \mathbf{w}_\epsilon(t,s) \tag{25}$$

where we have introduced the deviation vector $\mathbf{w}_\epsilon(t,s)$ arising from residual term in (23). Note that as $\mathbf{w}_\epsilon(t,s)$ involves a different value of t_ϵ at each τ, it does not have a simple expression; rather, $\mathbf{w}_\epsilon(t,s)$ must be bounded as in [8], but this is outside the scope of this paper. Instead we make the simple assumption that in the vicinity of the ridge,

$$\frac{\mathbf{w}_\epsilon(t,s)}{\|\mathbf{w}_\psi(t,s)\|} \approx 0 \tag{26}$$

which implies a constraint on the joint properties of the signal and the wavelet, see [8]. The transform modulus is then

$$\|\mathbf{w}_\psi(t,s)\| \approx \frac{1}{2}\|\mathbf{x}_+(t)\|\,\left|\Psi\left(s\omega_{\mathbf{x}}(t)\right)\right| \tag{27}$$

so the solution to the amplitude ridge equation is

$$s^{\{a\}}(t) \approx \frac{\omega_\psi}{\omega_{\mathbf{x}}(t)} \tag{28}$$

and we have

$$\widehat{\mathbf{x}}^{\{a\}}_{+;\psi}(t) = \mathbf{w}_\psi\Big(t, \widehat{s}^{\{a\}}(t)\Big) \approx \mathbf{x}_+(t) \quad t \in T^{\{a\}} \tag{29}$$

for the form of the ridge-based signal estimate. It is clear that the signal may be accurately recovered when the modulation strength is sufficiently small and when the frequencies of the components are sufficiently close together.

It is important to note that the multivariate wavelet ridge analysis is invariant to unitary transformations of the transform vector. That is, transforming $\mathbf{w}_\psi(t,s)$ as $\mathbf{U}\mathbf{w}_\psi(t,s)$ for some unitary matrix $\mathbf{U}$, the solutions to (17–18) remain unchanged. For bivariate and trivariate signals, such transformations include real rotations of $\mathbf{x}(t)$, as well as changes in the polarization state of the signal from linear motion to circular motion [9]. By contrast no such invariance property is possessed by the method of [4], in which one separately finds the univariate ridges of the individual signal components, essentially requiring a particular polarization state to be specified *a priori*.

IV. Application

An application will now be presented to the dataset shown in Fig. 1a. The data consists of acoustically-tracked subsurface oceanographic floats [16], which drift with the ocean currents at a chosen depth level, in this case about 1000 m. Freely-drifting float data such as these represent one of the primary ways oceanographers study large-scale ocean currents. This dataset is from the "Eastern Basin" experiment [17], an early experiment with this type of instrument. The data is available online from the World Ocean Circulation Experiment Subsurface Float Data Assembly Center at http://wfdac.whoi.edu. Here 27 different time series are plotted, each corresponding to a distinct float. The sample rate is one day, and only float records containing greater than 200 data points are presented.

The observed float data presented in Fig. 1a is bivariate in that we have a set of real-valued time series pairs,

$$\mathbf{x}^{(o)}(t) = \begin{bmatrix} x^{(o)}(t) \\ y^{(o)}(t) \end{bmatrix} \tag{30}$$

where $x^{(o)}(t)$ represents the observed east-west displacement and $y^{(o)}(t)$ the north-south displacement; these are converted to units of kilometers for computational purposes with a Cartesian expansion about the point 30° N, 25° W. Some trajectories—those shown with black curves—present tightly looping trajectories and so appear to contain modulated oscillations, while the remainder have a more chaotic appearance.

In the oceanographic community it is well known that such looping trajectories in these [4], [17] and other float records are characteristic signatures of oceanic vortices; see e.g. [4]

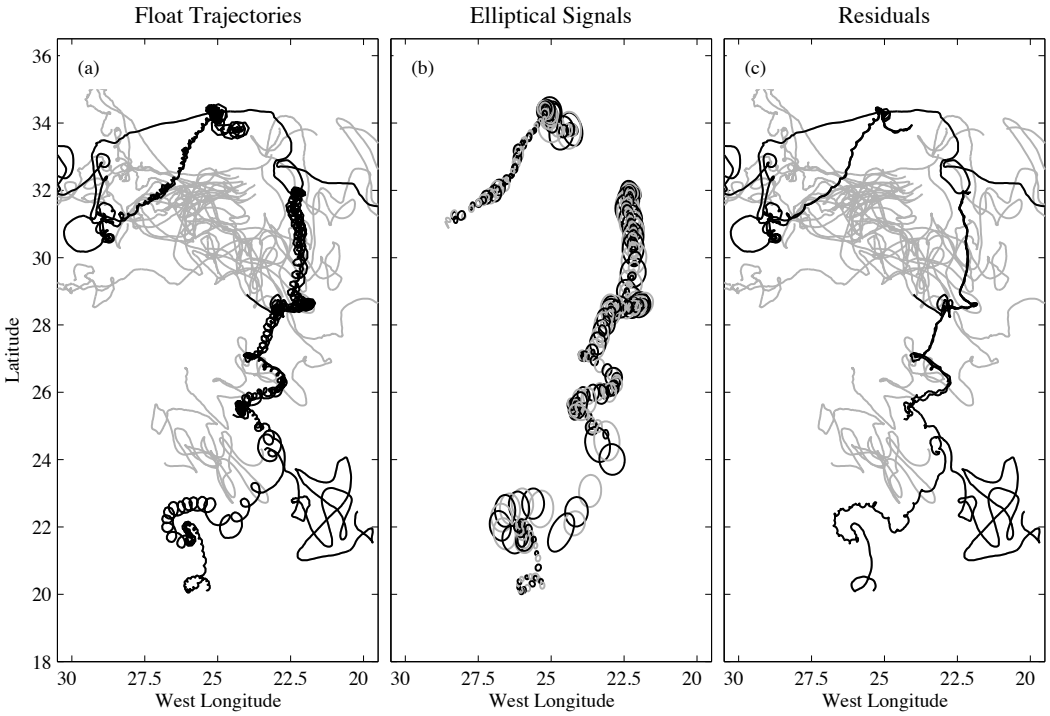

Fig. 1. Multivariate wavelet ridge analysis applied to oceanographic data. Panel (a) shows a set of position records from 27 freely drifting subsurface oceanographic floats in the eastern subtropical Atlantic. The original data (a) is decomposed into a set of modulated bivariate oscillations, represented in (b) as snapshots of ellipses at successive times, together with the residuals shown in (c). The ellipses alternate between black and gray, and are shown at twice actual size for clarity. Time series for which a modulated oscillation is detected are plotted in (a) and (c) as black lines, while others are plotted as gray lines.

for further discussion. The observed signal is well described by the model

$$\mathbf{x}^{(o)}(t) = \mathbf{x}(t) + \mathbf{x}^{(\varepsilon)}(t) \tag{31}$$

where the modulated oscillation $\mathbf{x}(t)$ reflects the possible presence of a vortex, while the background flow and measurement noise is modeled by the stochastic signal $\mathbf{x}^{(\varepsilon)}(t)$. Since the physical properties of the vortices themselves are of interest, it is desirable to decompose the flow into a modulated oscillation plus a residual, as is accomplished by the ridge analysis.

For wavelets, we use the generalized Morse wavelets [14], [18], which are controlled by two parameters, γ and β. We use the choice $\gamma = 3$ since this leads to particularly attractive wavelet properties, see [14]. The wavelet transform

$$\mathbf{w}_\psi(t,s) = \begin{bmatrix} W_{x;\psi}(t,s) \\ W_{y;\psi}(t,s) \end{bmatrix} = \begin{bmatrix} \int_{-\infty}^{\infty} \frac{1}{s}\, \psi^*\left(\frac{\tau - t}{s}\right) x^{\{o\}}(\tau)\, d\tau \\ \int_{-\infty}^{\infty} \frac{1}{s}\, \psi^*\left(\frac{\tau - t}{s}\right) y^{\{o\}}(\tau)\, d\tau \end{bmatrix} \tag{32}$$

is here a bivariate function of time and scale. The multivariate ridge algorithm is then applied, and we reject ridges fewer than $2\sqrt{\beta\gamma}$ oscillations in length. The quantity $\sqrt{\beta\gamma}$ was shown by [14] to be a measure of the time-domain wavelet duration. Rejection of short ridges is advisable since we find from experience that noise tends to introduce spurious ridges of duration comparable to that of the wavelet. Apart from a small percentage of time points, these settings lead to either zero or one ridge present in each signal vector at any time.

The exact algorithms and settings may be found online in the freely distributed software package JLAB, available at the first author's web site http://www.jmlilly.net. The script `makefigs_asilomar` generate the figures in this paper by calling other JLAB functions, especially `morsewave` to compute the generalized Morse wavelets, `wavetrans` to implement the wavelet transform, `ridgewalk` to compute the wavelet ridges, and also `ellipseplot` to plot ellipses as in Fig. 1b. For most of the time series we use identical scale levels and the generalized Morse parameter β set to $\beta = 3$. However, for two of the float trajectories we use $\beta = 8$ and also different scale levels, in order to recover the higher-frequency variability present in those two trajectories.

An example of the multivariate wavelet ridge analysis is presented in Fig. 2 for one of the float trajectories. This time series corresponds in Fig. 1a to the strongly curving trajectory that extends from about 20° N to about 24° N, centered around 25° W. In Fig. 2a, the position time series has been differentiated to give a velocity time series for presentation. The presence of modulated oscillation in both signal components is readily apparent. Fig. 2b then shows

$$\|\mathbf{w}_\psi(t,s)\| = \sqrt{|W_{x;\psi}(t,s)|^2 + |W_{y;\psi}(t,s)|^2} \tag{33}$$

a maximum of which, by definition, is an amplitude ridge. The ridge algorithm gives the black curve extending over the entire duration of the time series, following the variability of the oscillation as it changes in frequency by an order of magnitude. The bivariate transform $\mathbf{w}_\psi(t,s)$ evaluated along this curve as in (20) is an estimate of the bivariate modulated oscillation.

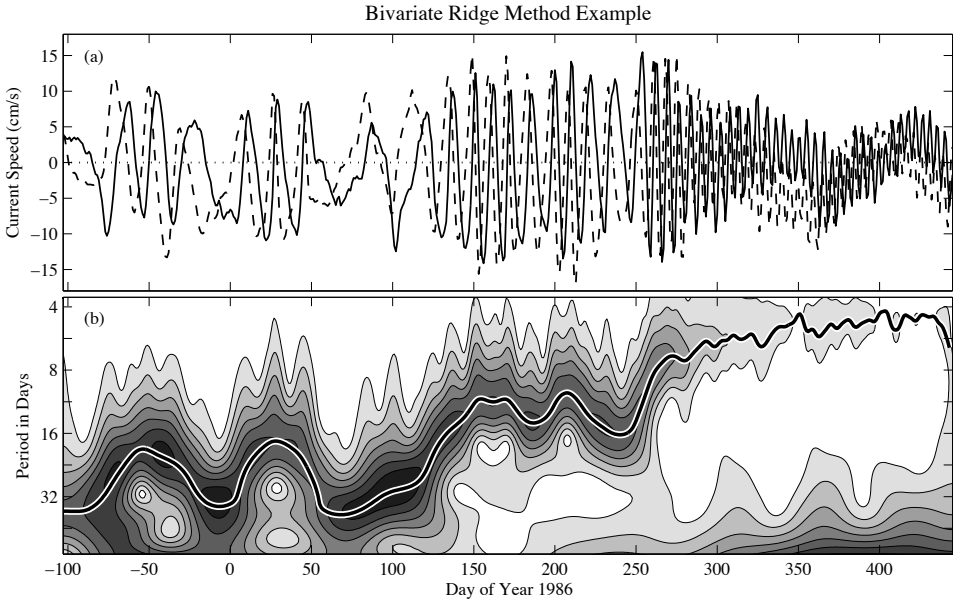

Fig. 2. Example of multivariate wavelet ridge analysis. A bivariate position signal, differentiated in time for presentational clarity, is plotted in (a). The solid curve represent eastward velocity and the dashed curve northward velocity. The norm of the bivariate wavelet transform $\mathbf{w}_\psi(t,s)$ of the position signal, shown in (b), has units of kilometers. The y-axis is logarithmic and shows the scale of the wavelet transform expressed in periods, $2\pi s/\omega_\psi$, with units of days. The contours range from 0 km to 65 km with a spacing of 5km. The heavy curve is a single unbroken ridge resulting from the amplitude ridge algorithm.

Applying the wavelet ridge algorithm to the entire data set shown in Fig. 1a leads to a set of estimated modulated bivariate oscillations $\widehat{\mathbf{x}}_+(t)$. Snapshots of these are plotted as ellipses in Fig. 1b, using the results of [9] to convert each complex-valued signal $\widehat{\mathbf{x}}_+(t)$ into the parameters of a time-varying ellipse. The time spacing between ellipse snapshots is in proportion to the estimated period of the modulated oscillation, with one ellipse plotted per period. The residual between estimated modulated oscillations $\Re\{\widehat{\mathbf{x}}_+(t)\}$, and the observed time series $\mathbf{x}^{\{o\}}(t)$, is shown in Fig. 1c. This residual primarily reflects the background flow and is seen to be largely devoid of the looping high-frequency variability. Thus the algorithm appears to have effectively partitioned the signal into a set of modulated oscillations plus a residual.

V. Conclusion

This paper has presented a simple idea for generalizing wavelet ridge analysis to the multivariate case. The method is expected to have small bias when the evolution of the signal components is comparable to that of a set of sinusoids all oscillating at the same frequency, and is independent of orthogonal transforms of the signal vector. An application to set of about two dozen oceanographic instruments is presented, with good results, illustrating that the multivariate ridge analysis is a promising methodology.

References

[1] B. Picinbono, "On instantaneous amplitude and phase of signals," *IEEE T. Signal Proces.*, vol. 45, pp. 552–560, 1997.

[2] N. Delprat, B. Escudié, P. Guillemain, R. Kronland-Martinet, P. Tchamitchian, and B. Torrésani, "Asymptotic wavelet and Gabor analysis: Extraction of instantaneous frequencies," *IEEE T. Inform. Theory*, vol. 38, no. 2, pp. 644–665, 1992.

[3] S. Mallat, *A wavelet tour of signal processing, 2nd edition*. New York: Academic Press, 1999.

[4] J. M. Lilly and J.-C. Gascard, "Wavelet ridge diagnosis of time-varying elliptical signals with application to an oceanic eddy," *Nonlinear Proc. Geoph.*, vol. 13, pp. 467–483, 2006.

[5] J. Park, F. L. V. III, and C. R. Lindberg, "Frequency-dependent polarization analysis of high-frequency seismograms," *J. Geophys. Res.*, vol. 92, pp. 12,664–12,674, 1987.

[6] J. M. Lilly and J. Park, "Multiwavelet spectral and polarization analysis," *Geophys. J. Int.*, vol. 122, pp. 1001–1021, 1995.

[7] S. C. Olhede and A. T. Walden, "Polarization phase relationships via multiple Morse wavelets. II. Data analysis," *P. Roy. Soc. Lond. A Mat.*, vol. 459, no. A, pp. 641–657, 2003.

[8] J. M. Lilly and S. C. Olhede, "On the analytic wavelet transform," *IEEE T. Inform. Theory*, 2009, submitted; available at http://arxiv.org/abs/0711.3834.

[9] ——, "Bivariate instantaneous frequency and bandwidth," *IEEE T. Signal Proces.*, 2009, in press.

[10] D. Gabor, "Theory of communication," *Proc. IEE*, vol. 93, pp. 429–457, 1946.

[11] H. B. Voelcker, "Toward a unified theory of modulation. I. Phase-envelope relationships." *Proc. IEEE*, vol. 54, pp. 340–353, 1966.

[12] B. Boashash, "Estimating and interpreting the instantaneous frequency of a signal—Part I: Fundamentals," *Proc. IEEE*, vol. 80, no. 4, pp. 520–538, 1992.

[13] M. Holschneider, *Wavelets: an analysis tool*. Oxford: Oxford University Press, 1998.

[14] J. M. Lilly and S. C. Olhede, "Higher-order properties of analytic wavelets," *IEEE T. Signal Proces.*, vol. 57, no. 1, pp. 146–160, 2009.

[15] M. Abramowitz and I. A. Stegun, *Handbook of Mathematical Functions with Formulas, Graphs, and Mathematical Tables*, tenth printing ed. National Bureau of Standards, 1972.

[16] H. T. Rossby, D. Dorson, and J. Fontain, "The RAFOS system," *J. Atmos. Ocean Tech.*, vol. 3, pp. 672–679, 1986.

[17] P. Richardson, D. Walsh, L. Armi, M. Schröder, and J. F. Price, "Tracking three Meddies with SOFAR floats," *J. Phys. Oceanogr.*, vol. 19, pp. 371–383, 1989.

[18] S. C. Olhede and A. T. Walden, "Generalized Morse wavelets," *IEEE T. Signal Proces.*, vol. 50, no. 11, pp. 2661–2670, 2002.